

IMAGE DATA ANALYSIS (6CFU)

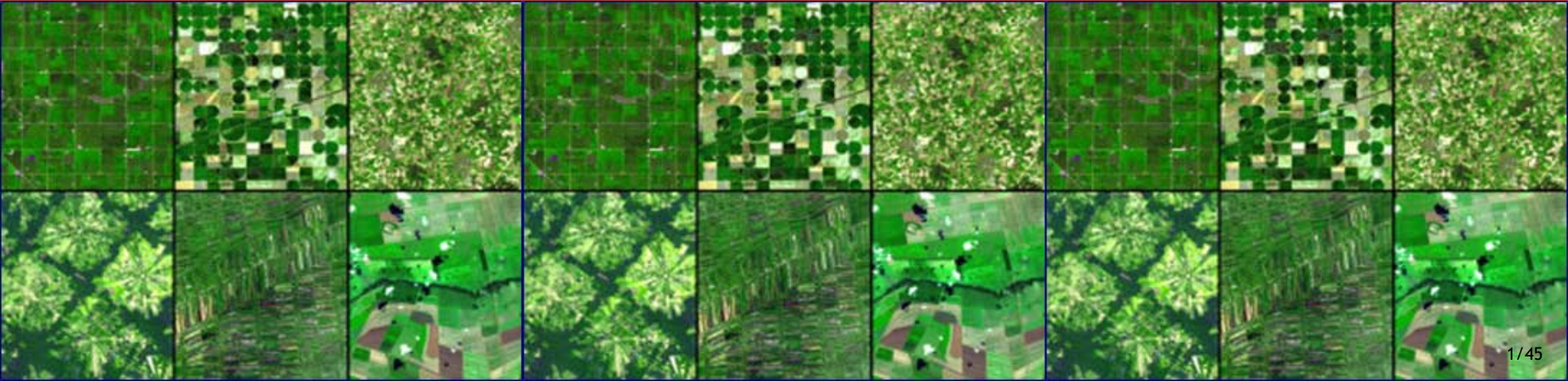
MODULE OF
REMOTE SENSING
(9 CFU)

A.Y. 2022/23

MASTER OF SCIENCE IN COMMUNICATION TECHNOLOGIES AND MULTIMEDIA
MASTER OF SCIENCE IN COMPUTER SCIENCE, LM INGEGNERIA INFORMATICA

PROF. ALBERTO SIGNORONI

ERROR CORRECTION AND REGISTRATION OF IMAGE DATA



Sources of error in Remote Sensing data



- When image data is recorded by sensors on satellites and aircraft it can contain errors in geometry and in the measured brightness values of the pixels
 - *this can happen also for many other professional fields of application at various scales: industrial, biomedical, cultural heritage, submarine, microscopy,...*
- Brightness errors are referred to as **radiometric errors** and can result
 - from the **instrumentation** used to record the data,
 - from the **wavelength dependence** of solar radiation and
 - from the **effect of the atmosphere**.
- Image **geometry errors** can arise in many ways.
 - The **relative motions** of the **platform**, its **scanners** and the **earth**, for example, can lead to errors of a skewing nature in an image product.
 - **Non-idealities in the sensors** themselves, the **curvature of the earth** and **uncontrolled position and altitude variations** of the remote sensing platform can all lead to geometric errors of varying degrees of severity.
- For many applications only the major sources of error will require compensation whereas in others more precise correction will be necessary.

Types of radiometric distortion

- ❑ Mechanisms that affect the measured brightness values of the pixels in an image can lead to two broad types of radiometric distortion.

1. **Intra-band:** the **relative distribution of brightness** over an image in a given band can be different to that in the **ground scene**.
2. **Inter-band:** the **relative brightness of a single pixel from band to band** can be distorted compared with the **spectral reflectance character of the corresponding region on the ground**.

- ❑ Both types can result from the presence of the atmosphere as a transmission medium through which radiation must travel from its source to the sensors, and can be a result also of instrumentation effects.

Absorption and scattering by the atmosphere

- **Absorption** by atmospheric molecules is a selective process that converts incoming energy into heat.
 - In particular, molecules of oxygen, carbon dioxide (CO_2), ozone (O_3), and water attenuate the radiation *very strongly in certain wavebands*.
 - Sensors commonly used in solid earth and ocean remote sensing are usually designed to *operate away from these regions* so that the effects are small.
- **Scattering** by atmospheric particles is then the dominant mechanism that leads to radiometric distortion in image data (apart from sensor effects).
- There are two broadly identified scattering mechanisms.
 1. The first is scattering by the air molecules themselves. This is called **Rayleigh scattering** and is an *inverse fourth power function of the wavelength* used.
 2. The other is called **aerosol or Mie scattering** and is a result of scattering of the radiation from *larger particles such as those associated with smoke, haze and fumes (e.g. from cars)*. These particulates are of the order of *one tenth to ten wavelengths*.
- Mie scattering is also wavelength dependent, although not as strongly as Rayleigh scattering. When the atmospheric particulates become much larger than a wavelength, such as those common in fogs, clouds and dust, the wavelength dependence disappears.



Absorption and scattering by the atmosphere

- In a clear ideal atmosphere Rayleigh scattering is the only mechanism present.
 - It accounts for example, for the blueness of the sky. Because the shorter (blue) wavelengths are scattered more than the longer (red) wavelengths we are more likely to see blue when looking in any direction in the sky.
 - Likewise the reddish appearance of sunset is also caused by Rayleigh scattering. This is a result of the long atmospheric path the radiation has to follow at sunset during which most short wavelength radiation is scattered away from direct line of sight by comparison to the longer wavelengths.
- In contrast to Rayleigh scattering, fogs and clouds appear white or bluish-white owing to the (near) non-selective scattering caused by the larger particles.



We are now in the position to “appreciate” the effect of the atmosphere on the radiation that ultimately reaches a sensor.

Atmospheric Effects on Remote Sensing Imagery

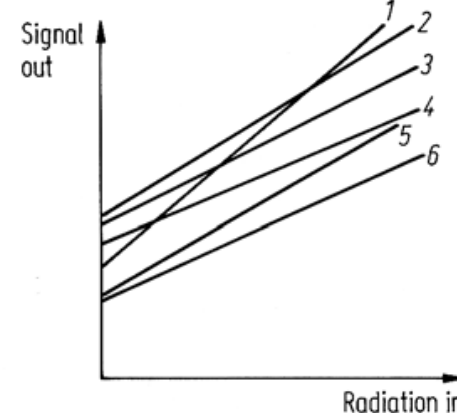
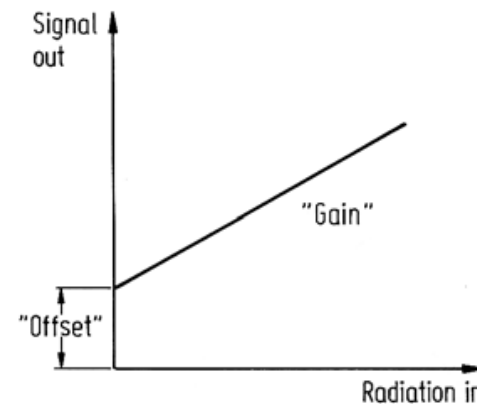


- A result of the scattering caused by the atmosphere is that **fine detail in image data will be obscured**. Consequently, it is important in applications where one is dependent upon the limit of sensor resolution available, such as in *urban studies*, to take steps to correct for atmospheric effects.
- It is important also to consider carefully the effects of the atmosphere on remote sensing systems with wide fields of view in which there will be an appreciable **difference in atmospheric path length** between nadir and the extremities of the swath.
- Finally, and perhaps most importantly, because both Rayleigh and Mie scattering are wavelength dependent, **the effects of the atmosphere will be different in the different wavebands** of a given sensor system.
 - In the case of the Landsat Thematic Mapper the visible blue band (0.45 to 0.52 μm) can be affected appreciably by comparison to the middle infrared band (1.55 to 1.75 μm).
 - This leads to a loss in calibration of the set of brightnesses associated with a particular pixel.

Instrumentation Errors

- Radiometric errors within a band and between bands can also be caused by the design and operation of the **sensor system**. 
- Band to band errors from this source are normally ignored by comparison to band to band errors from atmospheric effects. However, **detector system errors** within a band can be quite severe and often **require correction** to render an image product useful.
- An ideal radiation detector should have a **linear transfer characteristic**. However real detectors will have some degree of nonlinearity (ignored here) and will also give a small signal out (dark current offset), see Figure (a), even when no radiation is being detected.
- Whiskbroom (raster scan) remote sensors involve a **multitude of detectors**. In the case of the Landsat MSS there were 6 per band, for the Landsat TM there are 16 per band.
- Pushbroom detectors (linear cameras) can have hundreds to thousands of receptors in the swath direction.
- Each of these detectors will have slightly different transfer characteristics, as described by their gains and offsets, as shown in Figure (b). This could cause **image striping artifacts** either in the along swath direction (whiskbroom scanning) or in the across swath direction (for pushbroom scanning).

Whiskbroom vs Pushbroom
<https://svs.gsfc.nasa.gov/12754>



Correction of Atmospheric Effects



□ Detailed Correction of Atmospheric Effects

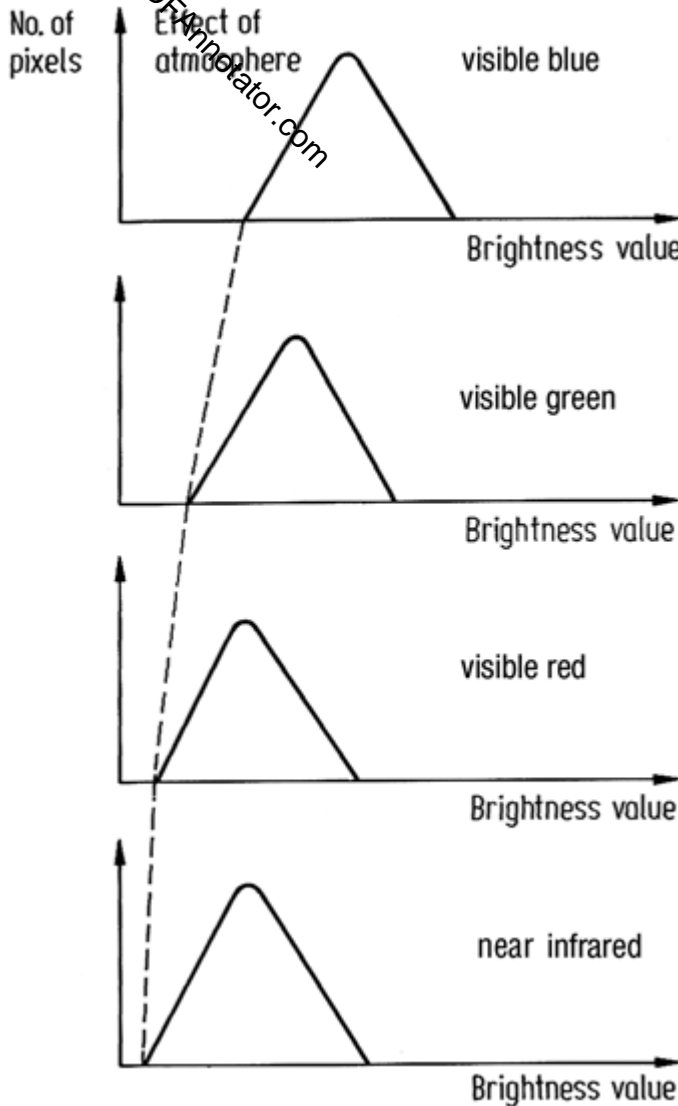
- See example on the textbook. The example is based on the precise knowledge of some ancillary information such as temperature, relative humidity, atmospheric pressure, visibility and solar zenith angle... and on the exploitation of an atmosphere effects model.

□ Bulk Correction of Atmospheric Effects

- In many cases detailed correction for the scattering and absorbing effects of the atmosphere is not required, and often the necessary ancillary information such as visibility and relative humidity is not readily available. In this case an approximate correction is typically carried out.
- If the effect of the atmosphere is judged to be a problem in imagery, approximate bulk correction can be carried out in the following manner.
 - First it is assumed that each band of data for a given scene should have contained some pixels at or close to zero brightness value but that atmospheric effects, and especially **path radiance, has added a constant value to each pixel in a band.**
 - Consequently if histograms are taken of each band the **lowest significant occupied brightness value will be non-zero.**
 - Moreover because path radiance varies as $\lambda^{-\alpha}$ (with α between 0 and 4 depending upon the extent of Mie scattering) the **lowest occupied brightness value will be further from the origin for the lower wavelengths** as depicted in the following Figure.

LOOK AT FOLLOWING SLIDE

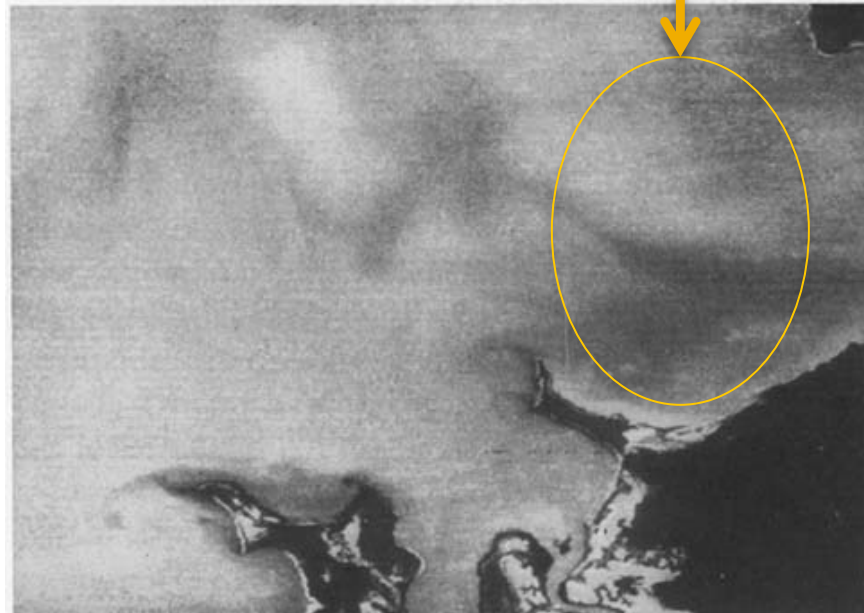
Correction of Atmospheric Effects



- **Correction** consists in
 - first to identifying the amount by which each histogram is “shifted” in brightness away from the origin
 - and then subtracting that amount from each pixel brightness in that band.
- It is clear that *the effect of atmospheric scattering as implied in the histograms of Figure is to lift the overall brightness value of an image in each band.*
 - In the case of a color composite product this will appear as a whitish-bluish haze.
 - Upon correction in the manner just described this haze will be removed and the dynamic range of image intensity will be improved.
 - Consequently, the procedure of atmospheric correction outlined in this section is frequently referred to as **haze removal.**

Correction of Instrumentation Errors

- Errors in relative brightness such as the within-band line striping referred above and shown in Figure can be rectified to a great extent.
- First it is assumed that the detectors used for data acquisition within a band produce signals statistically similar to each other.
- In other words if the means and standard deviations are computed for the signals recorded by the detectors then they should be the same (reasonable for whiskbroom detector arrays).
 - This requires the assumption that detail within a band doesn't change significantly over a distance equivalent to that of one scan covered by the set of the detectors (e.g. 474 m for the six scan lines of Landsats 1,2,3 MSS).
 - This is a reasonable assumption so that differences in those statistics among the detectors can be attributed to gain and offset mismatches, as discussed above (instrumentation errors slide).
 - These mismatches can be detected by calculating pixel brightness statistics using image data lines, which are known to come from a single detector. *Referred to as "destriping"*



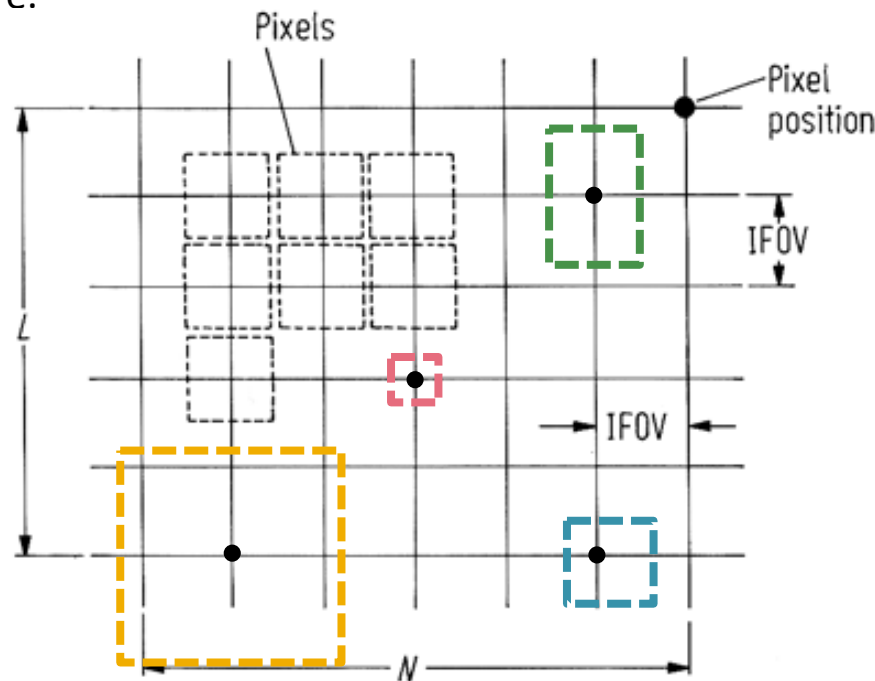
Sources of Geometric Distortion

- There are potentially many more sources of geometric distortion of image data than radiometric distortion and their effects are more severe.
- They can be related to a number of factors, including
 1. *the rotation of the earth during image acquisition,*
 2. *the finite scan rate of some sensors,*
 3. *the wide field of view of some sensors,*
 4. *the curvature of the earth,*
 5. *sensor non-idealities,*
 6. *variations in platform altitude, attitude and velocity, and*
 7. *panoramic effects related to the imaging geometry.*
- It is the purpose here to discuss the nature of the distortions that arise from these effects; later we will discuss means by which the distortions can be compensated.



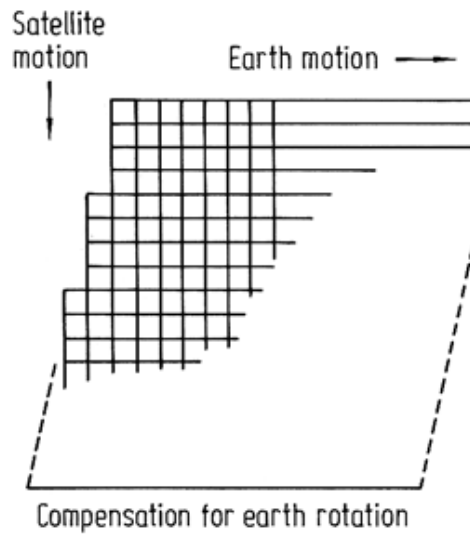
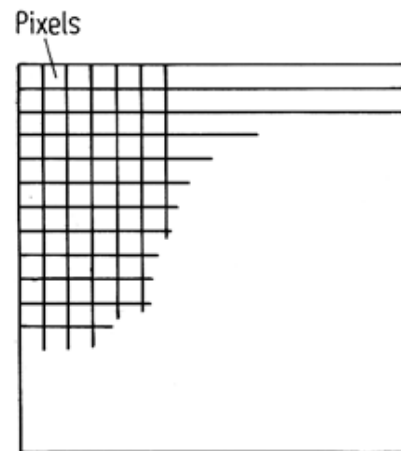
Basic image formation geometry

- To appreciate why geometric distortion occurs, in some cases it is necessary to envisage how an image is formed from sequential lines of image data.
 - If one imagines that a particular sensor records L lines of N pixels each then it would be natural to form the image by laying the L lines down successively one under the other.
 - The grid intersections are the pixel positions and, ideally, the spacing between those grid points is equal to the sensor's instantaneous field of view (IFOV).
 - If the IFOV of the sensor has an aspect ratio of unity – i.e. the pixels are the same size along and across the scan – then this is the same as arranging the pixels for display on a square grid, such as that shown in Figure.
 - However **unity aspect ratio** and pixel size equal to the grid spacing is not automatically granted in linear acquisitions (either raster scan or pushbroom).
 - The system should be **designed** to provide it, or to correct from possible distortion generated by wrong size or bad anisotropic aspect ratio of acquired pixels.
 - In figure different kind of possible distortions are exemplified.



Earth Rotation Effects

- Line scan sensors (such as the Landsat TM) take a finite time to acquire a frame of image data. The same is true of push broom scanners (such as the SPOT HRV).
- During the frame acquisition time the earth rotates from west to east
 - therefore if the lines of image data recorded were arranged for display in the manner of Figure (a), the later lines would be erroneously displaced to the east;
 - instead, to give the pixels their correct positions relative to the ground it is necessary to offset the bottom of the image to the west by the amount of movement of the ground during acquisition, with all intervening lines displaced proportionately as shown in Fig.(b).
 - this amount depends upon the relative velocities of the satellite and earth and the length of the image frame recorded.

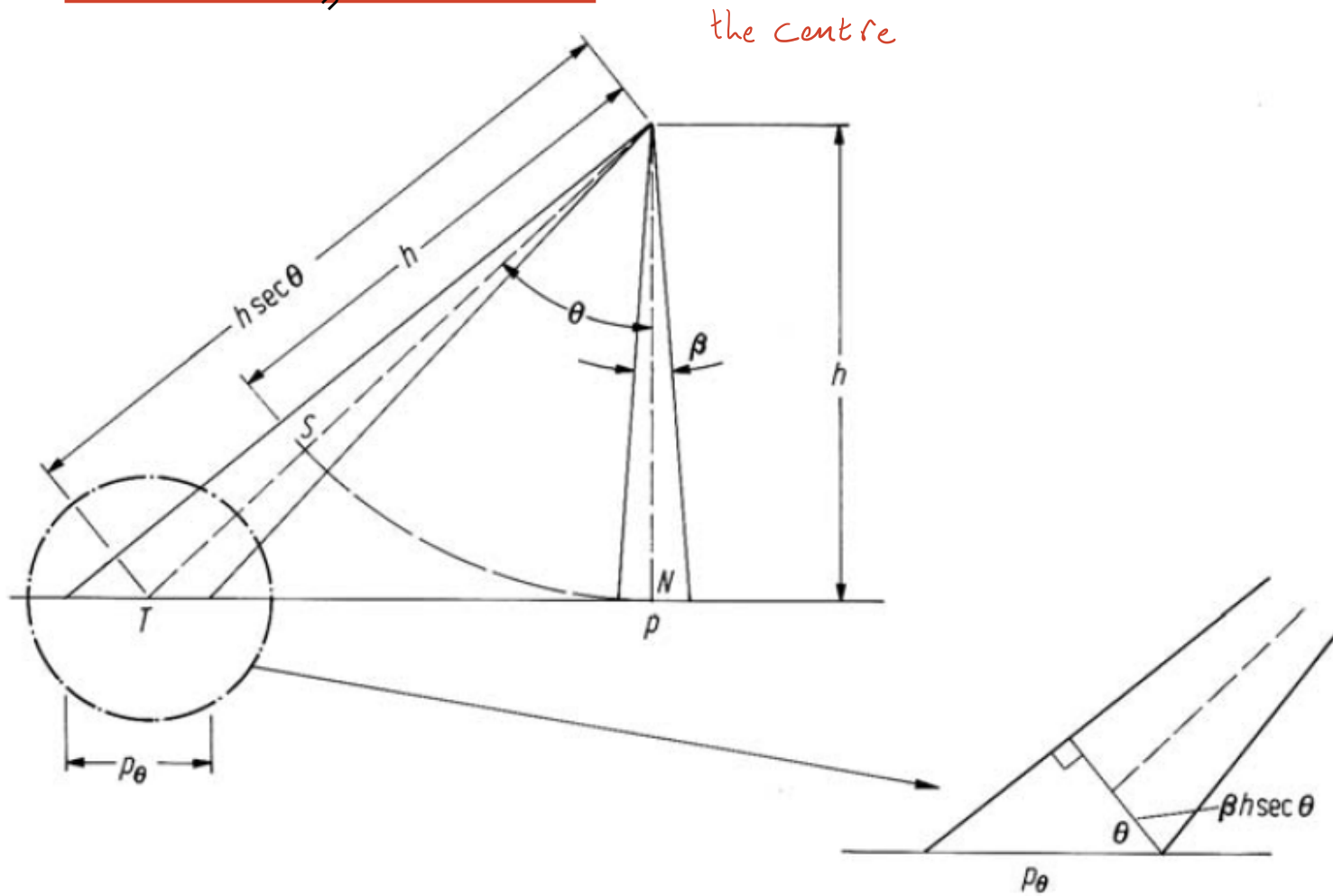


a

b

Panoramic Distortion

- For scanners used on spacecraft and aircraft remote sensing platforms the angularIFOV is constant. As a result the effective pixel size on the ground is larger at the extremities of the scan than at ~~nadir~~, as illustrated in Figure.



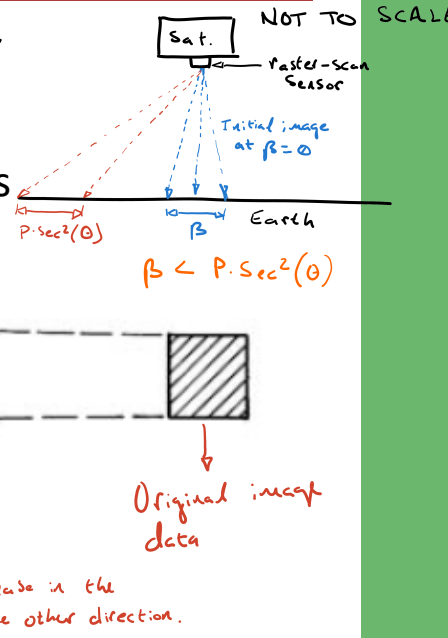
Panoramic Distortion

- In particular, if the IFOV is β and the pixel dimension at nadir is p then its **dimension in the scan direction** at a scan angle of θ as shown is

$$p_\theta = \beta h \sec^2 \theta = p \sec^2 \theta,$$

where h is altitude,

\star Remember IFOV is the dimen. of a given pixel whilst FOV is the sum dimen. of all pixels



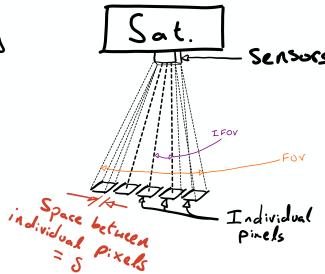
while its **dimension across the scan line** is $p \sec \theta$.

- For small values of θ these effects are negligible. For example, for Landsat 7 the largest value of θ is approximately 7.5° so that $p_\theta = 1.02 p$.
- However for systems with larger fields of view, such as [MODIS](#) and aircraft scanners, the effect can be quite severe.
- For an aircraft scanner with $\text{FOV} = 80^\circ$ the distortion in pixel size along the scan line is $p_\theta = 1.70 p$ – i.e. the region on the ground measured at the extremities of the scan is 70% larger laterally than the region sensed at nadir.
- When the image data is arranged on a regular grid, the displayed pixels are equal across the scan line whereas the equivalent ground areas covered are not.
- This gives a **geometric compression** of the image data towards its edges.

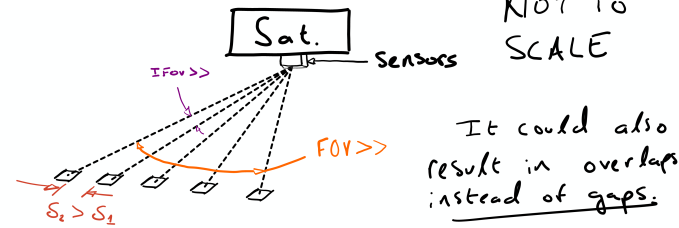
Panoramic Distortion

- There is a second distortion introduced with wide field of view systems and that relates to pixel positions across the scan line.
 - The scanner records pixels at constant angular increments, however the spacings of the effective pixels on the ground increase with scan angle.
 - For example if the pixels are recorded at an angular separation equal to the IFOV of the sensor then at nadir the pixels centres are spaced p apart. At a scan angle ϑ the pixel centres will be spaced $p \sec^2 \vartheta$ apart as can be ascertained from the above Figure.
- Thus by placing the pixels on a uniform display grid the image will suffer an across track compression.
 - Again the effect for small angular field of view systems will be negligible in terms of the relative spacing of adjacent pixels.
 - However when the effect is compounded to determine the location of a pixel at the swath edge relative to nadir the error can be significant.
 - This can be determined by computing the length of the arc $SN = \vartheta h$ in the above Figure, S being the position to which the pixel at T would appear to be moved if the data is arrayed uniformly.
 - It can be shown readily that $SN/TN = \vartheta / \tan \vartheta$ this being the degree of across track scale distortion.

Imagine we have a linear pixel array which also performs raster-scanning. We begin with an array and a slight gap (or overlap) between each pixel.

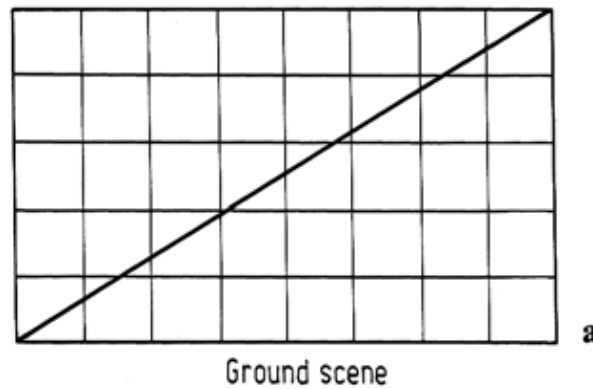


If we scan left or right this space will increase

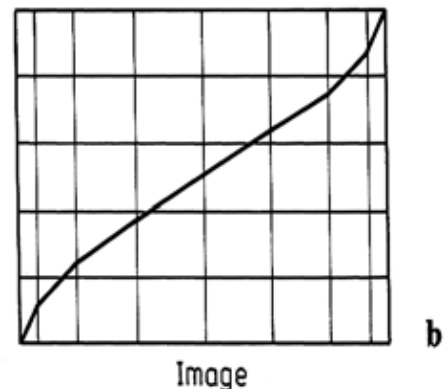


Panoramic Distortion

- These panoramic effects lead to an interesting distortion in the geometry of large field of view systems. To see this consider the uniform mesh shown in Figure (a).
 - Suppose this represents a region on the ground being imaged. For simplicity the cells in the grid could be considered to be features on the ground. Because of the **compression in the image data** caused by displaying equal-sized pixels on a uniform grid as discussed in the foregoing, the uniform mesh will appear as shown in Figure (b).
 - Image pixels are recorded with a constant IFOV and at a constant angular sampling rate. Therefore pixels near the swath edges will contain information in common owing to the **overlapping IFOV**.



a



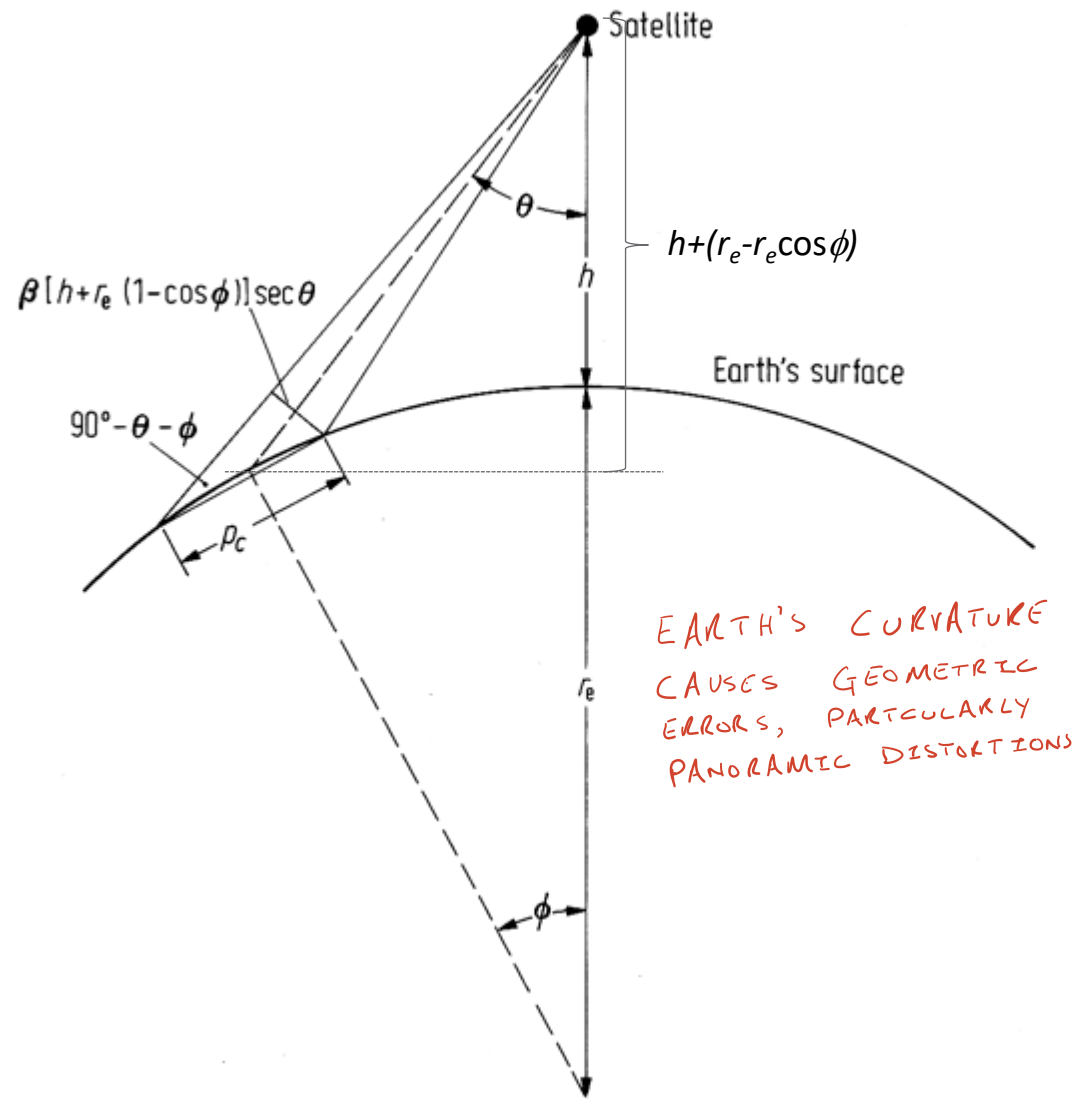
Image

b

- Linear features such as roads at an angle to the scan direction will appear bent in the displayed image data because of the compression effect. Owing to this, the distortion is also called **S-bend distortion** and can be a common problem with aircraft line scanners.
- Clearly, not only linear features are affected; rather the whole image detail near the swath edges is distorted in this manner.

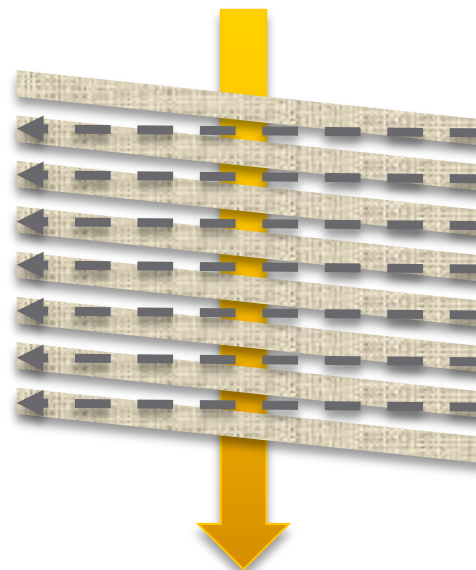
Earth Curvature

- Aircraft scanning systems, because of their low altitude (and thus the small absolute swath width of their image data), are not affected by earth curvature.
- Neither are space systems on LEO orbits, such as Landsat and SPOT, again because of the *narrowness of their swaths*.
- However, **wide swath width spaceborne imaging systems** are affected.
 - For MODIS with a swath width of 2330 km and an altitude of 705 km it can be shown that the deviation of the earth's surface from a plane amounts to less than 1% over the swath, which seems insignificant. *However it is the inclination of the earth's surface over the swath that causes the greater effect.*



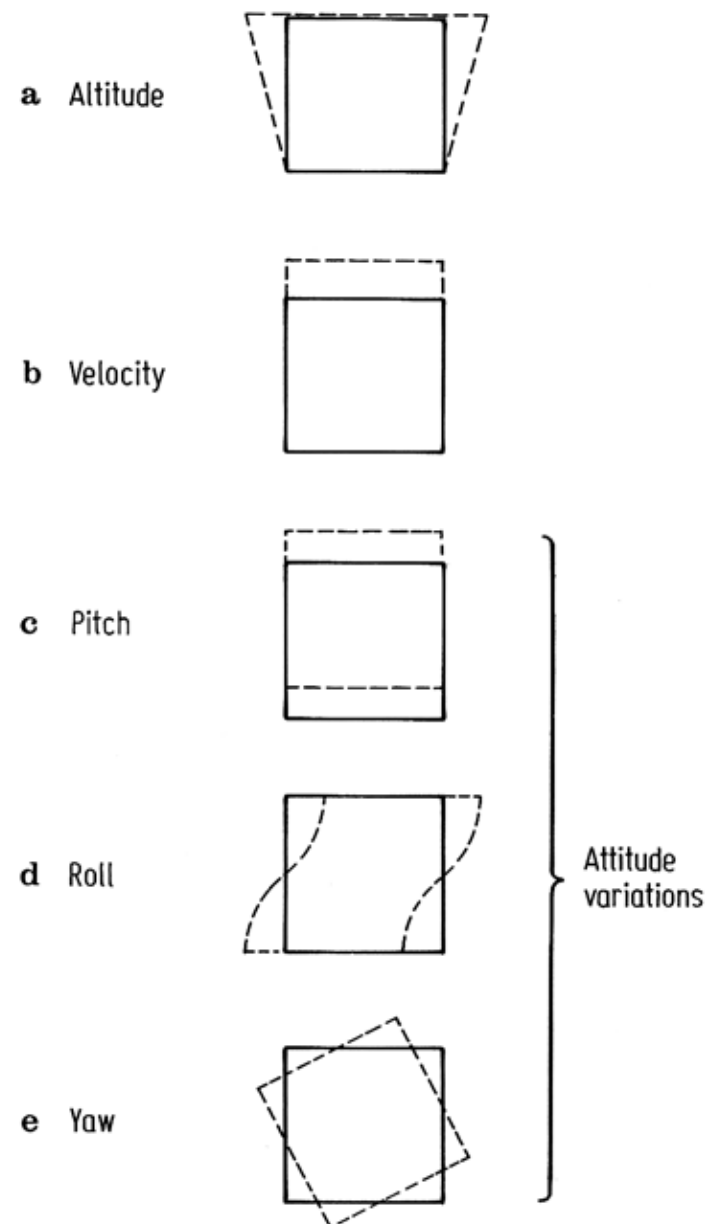
Scan Time Skew

- Mechanical line scanners such as the Landsat MSS and TM require a finite time to scan across the swath.
- During this time the satellite is moving forward leading to a skewing in the along track direction.
 - As an illustration of the magnitude of the effect, the time required to record one MSS scan line of data is 33 ms. During this time the satellite travels forward by 213 m at its equivalent ground velocity of 6.467 km s^{-1} .
 - As a result the end of the scan line is advanced by this amount compared with its start.



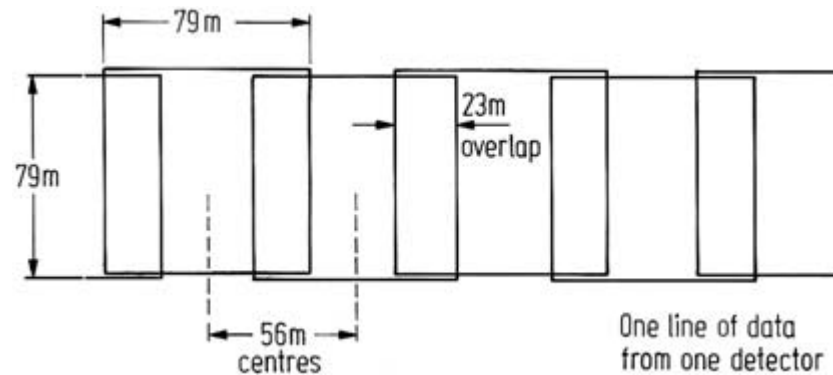
Variations in Platform Altitude, Velocity and Attitude

- **Variations in the elevation or altitude** of a remote sensing platform lead to a **scale change** at constant angular IFOV and field of view; the effect is illustrated in Fig.(a) for an increase in altitude with travel at a rate that is slow compared with a frame acquisition time.
- Similarly, if the platform forward **velocity changes**, a **scale change occurs** in the along track direction. This is depicted in Fig.(b) again for a change that occurs slowly. For a satellite platform, orbit velocity variations can result from orbit eccentricity and the non-sphericity of the earth.
- Platform **attitude changes** can be resolved into **yaw, pitch and roll** during forward travel. These lead to image rotation, along track and across track displacement as noted in Fig.(c–e).



Aspect Ratio Distortion

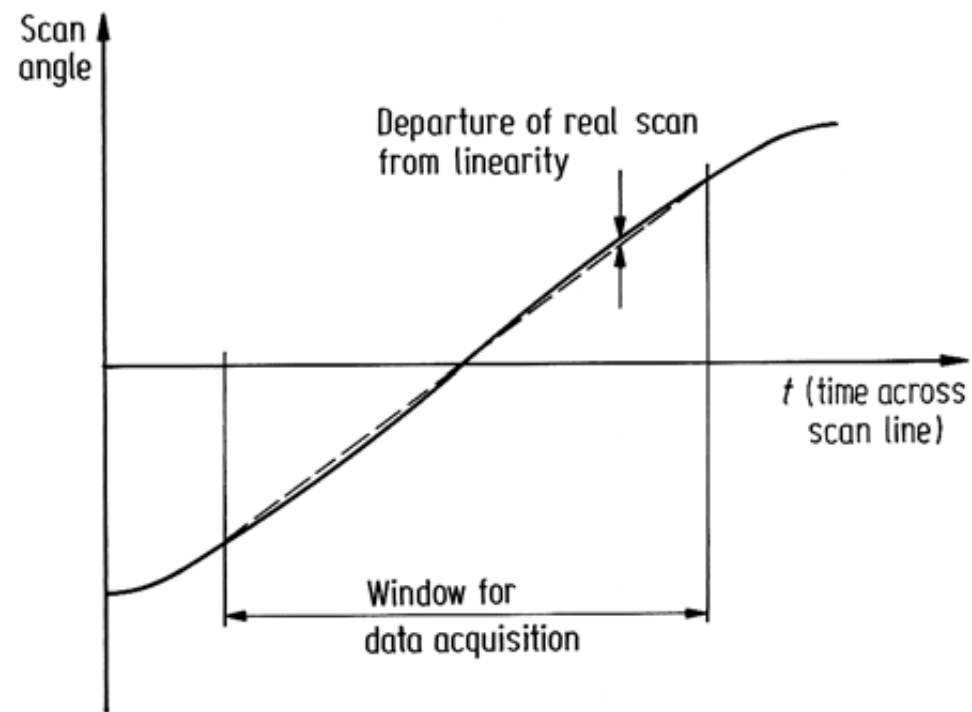
- The aspect ratio of an image (that is, its scale vertically compared with its scale horizontally) can be distorted by mechanisms that lead to overlapping IFOV's.
 - The most notable example of this occurs with the Landsat multispectral scanner, where samples are taken across a scan line too quickly compared with the IFOV. This leads to pixels having 56 metre centres but sampled with an IFOV of 79 m. Consequently the effective pixel size is $79 \text{ m} \times 56 \text{ m}$ and thus is not square (see Figure).
 - As a result, if the pixels recorded by the multispectral scanner are displayed on a regular grid the image will be too wide for its height when related to the corresponding region on the ground. The magnitude of the distortion is $79/56 = 1.411$ so that this is quite a severe error and *must be corrected* for most applications.



- A similar distortion can occur with aircraft scanners if the velocity of the aircraft is not matched to the scanning rate of the sensor. Either underscanning or overscanning can occur leading to distortion in the alongtrack scale of the image.

Sensor Scan Nonlinearities

- Line scanners that make use of rotating mirrors, such as the NOAA AVHRR and aircraft scanners, have a *scan rate across the swath that is constant*, to the extent that the scan motor speed is constant.
- Systems that use an **oscillating mirror** however, such as the Landsat thematic mapper, incur some **nonlinearity in scanning near the swath edges** owing to the need for the mirror to slow down and change directions.
 - This effect is depicted in Figure. This can lead to *a maximum displacement in pixel position compared with a perfectly linear scan of about 395 m*, for example, for Landsat multispectral scanner products.
 - Figure shows mirror displacement versus time in an oscillating mirror scanner system. Note that data acquisition does not continue to the extremes of the scan so that major nonlinearities are obviated.



Correction of Geometric Distortion – general aspects

- There are two approaches that can be used to correct the various types of geometric distortion present in digital image data.
 1. One is to **model the nature and magnitude of the sources of distortion** and use these models to establish correction formulae. This **technique is effective when the types of distortion are well characterized**, such as that caused by earth rotation.
 - Correction by mathematical modeling is discussed later.
 2. The second approach depends upon **establishing mathematical relationships between the position of pixels in an image and the corresponding coordinates of those points on the ground** (via a **map**). These relationships can be used to correct the image geometry irrespective of the analyst's **knowledge of the source and type of distortion**.
 - This procedure will be treated first since it is the most commonly used and, as a technique, is **general and independent of the platform/device** used for data acquisition.
- Before proceeding **it should be noted that each band of image data has to be corrected**. However, since it can often be assumed that the bands are well registered to each other, steps taken to correct one band in an image, can be used on all remaining bands.

Use of Mapping Polynomials for Image Correction

- An assumption that is made in this procedure is that there is available a map of the region corresponding to the image, that is correct geometrically.

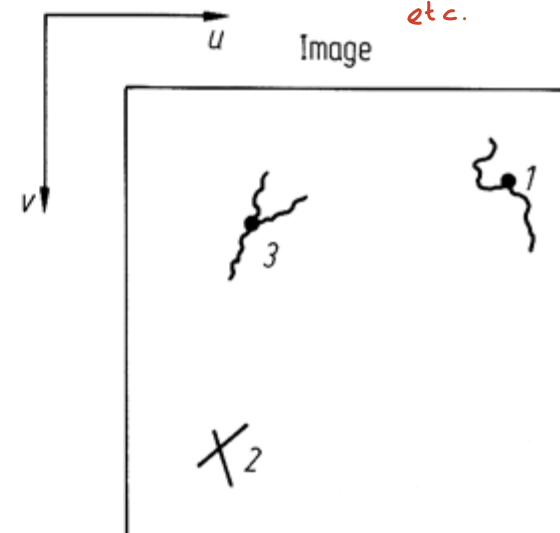
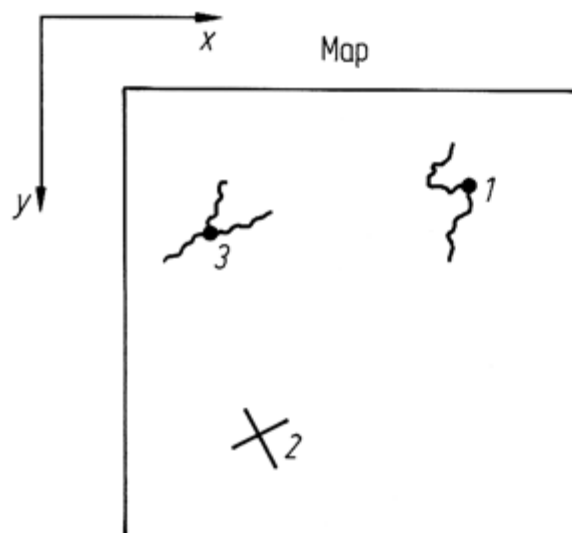
- We then define two Cartesian coordinate systems as shown in Figure.

Map data, $f(x, y)$ } Define a set of functions to relate:
 Image data, $f(u, v)$ } $u \longleftrightarrow (x, y)$
 $v \longleftrightarrow (x, y)$

This gives a set of polynomials with unknown coefficients: $\{a_i, b_i\}$

Using a set of matched/paired points from each data set or Ground Control Points (GCPs) we can estimate the values of the set $\{a_i, b_i\}$.

GCPs are usually easily identifiable landmarks, buildings etc.



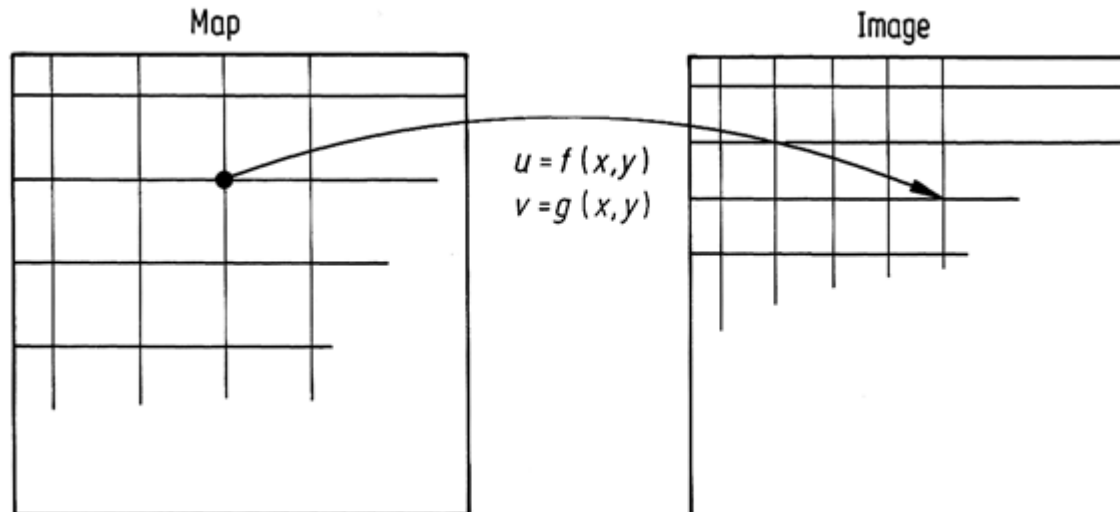
In reality a least squares estimation algorithm is used so that significant distortions don't affect this process.

Also many more GCPs than theoret. required are used to mitigate any issues.

Use of Mapping Polynomials for Image Correction

Resampling

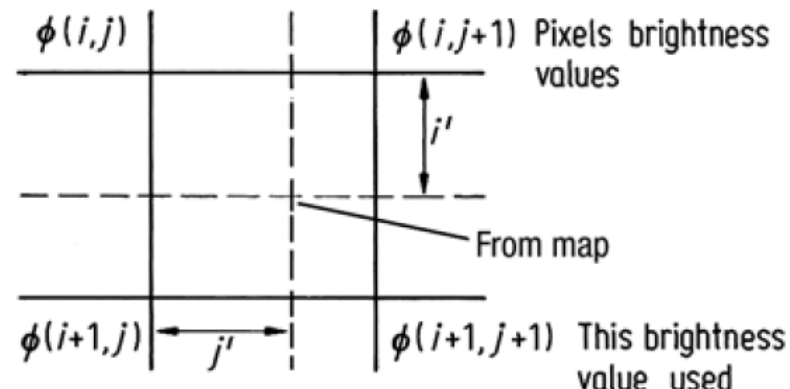
- Having determined the mapping polynomials explicitly by use of the ground control points, the next step is to find points in the image corresponding to each location in the pixel grid previously defined over the map.
 - The spacing of that grid is chosen according to the pixel size required in the corrected image and need not be the same as that in the original geometrically distorted version.
 - For the moment suppose that the points located in the image correspond exactly to image pixel centres. Then those pixels are simply transferred to the appropriate locations on the display grid to build up the rectified image. This is the case in Figure.



Use of Mapping Polynomials for Image Correction

Interpolation

- As is to be expected, grid centres from the map-registered pixel grid will not usually project to exact pixel centre locations in the image, as shown in the above Figure, and some decision has to be made therefore about what pixel brightness value should be chosen for placement on the new grid.
 - Three techniques can be used for this purpose.
1. ***Nearest neighbor resampling*** simply chooses the actual pixel that has its centre nearest the point located in the image, as depicted in Figure. This pixel is then transferred to the corresponding display grid location. This is the preferred technique if the new image is to be classified since it then consists of the original pixel brightnesses, simply rearranged in position to give a correct image geometry.



Use of Mapping Polynomials for Image Correction

Interpolation

2. **Bilinear interpolation** uses three linear interpolations over the four pixels that surround the point found in the image corresponding to a given display grid position.

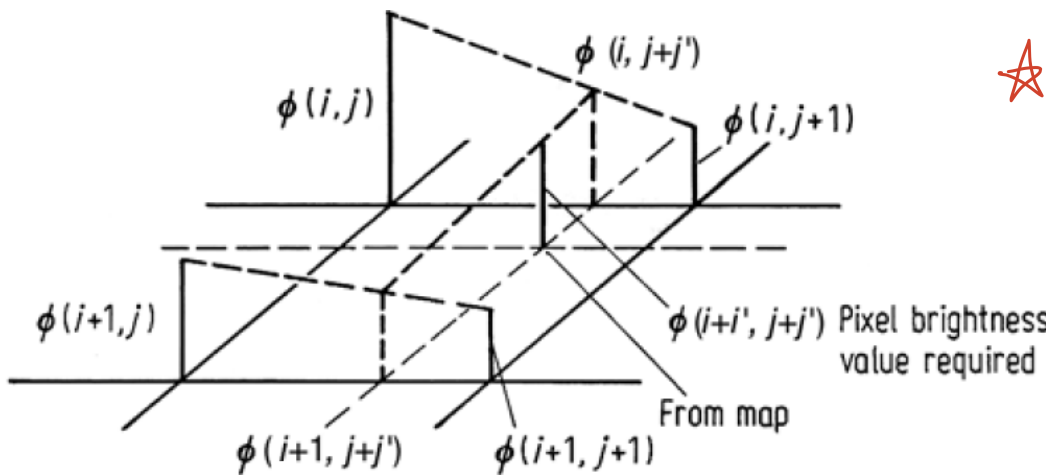
- The process is illustrated in Figure: Two linear interpolations are performed along the scan lines to find the interpolants $\phi(i, j + j')$ and $\phi(i + 1, j + j')$ as shown.
- These are given by $\phi(i, j + j') = j'\phi(i, j + 1) + (1 - j')\phi(i, j)$

$$\phi(i + 1, j + j') = j'\phi(i + 1, j + 1) + (1 - j')\phi(i + 1, j)$$

where ϕ is pixel brightness and $(i+i', j+j')$ is the position at which an interpolated value for brightness is required. The position is measured with respect to (i, j) and assumes a grid spacing of unity in both directions. The final step is to interpolate linearly over $\phi(i, j + j')$ and $\phi(i + 1, j + j')$ to give $\phi(i + i', j + j') = (1 - i')\{\phi(i, j + 1) + (1 - j')\phi(i, j)\} + i'\{\phi(i + 1, j + 1) + (1 - j')\phi(i + 1, j)\}$

$$+ i'\{\phi(i + 1, j + 1) + (1 - j')\phi(i + 1, j)\}$$

★ Recap linear interpolation

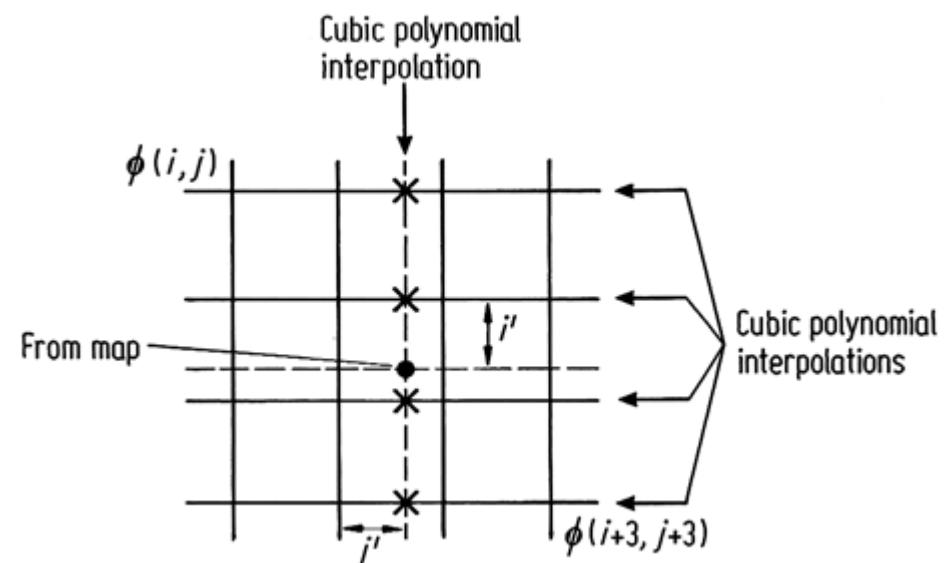


Use of Mapping Polynomials for Image Correction

Interpolation

- **Cubic convolution interpolation** uses the surrounding sixteen pixels.

- Cubic polynomials are fitted along the four lines of four pixels surrounding the point in the image, as depicted in Figure to form four interpolants.
- A fifth cubic polynomial is then fitted through these to synthesize a brightness value for the corresponding location in the display grid.
- The actual form of polynomial that is used for the interpolation is derived from considerations in sampling theory and issues concerned with constructing a continuous function (i.e. interpolating) from a set of samples.
- An excellent treatment of the problem has been given by Shlien (1979), who discusses several possible cubic polynomials that could be used for the interpolation process and who also demonstrates that the interpolation is a convolution operation.
- Based on the choice of a suitable polynomial (attributable to Simon (1975)) the algorithm that is used to perform cubic convolution interpolation is (Moik, 1980): →



Use of Mapping Polynomials for Image Correction

Interpolation

$$\rightarrow \phi(i, j + 1 + j') = j' \{ j' [\phi(i, j + 3) - \phi(i, j + 2) + \phi(i, j + 1) - \phi(i, j)] \\ + [\phi(i, j + 2) - \phi(i, j + 3) - 2\phi(i, j + 1) + 2\phi(i, j)] \\ + [\phi(i, j + 2) - \phi(i, j)] \} \\ + \phi(i, j + 1)$$

- This expression is evaluated for each of the four lines of four pixels depicted in Figure, to yield the four interpolants $\phi(i, j + 1 + j')$, $\phi(i + 1, j + 1 + j')$, $\phi(i + 2, j + 1 + j')$, $\phi(i + 3, j + 1 + j')$.
- These are then interpolated vertically according to

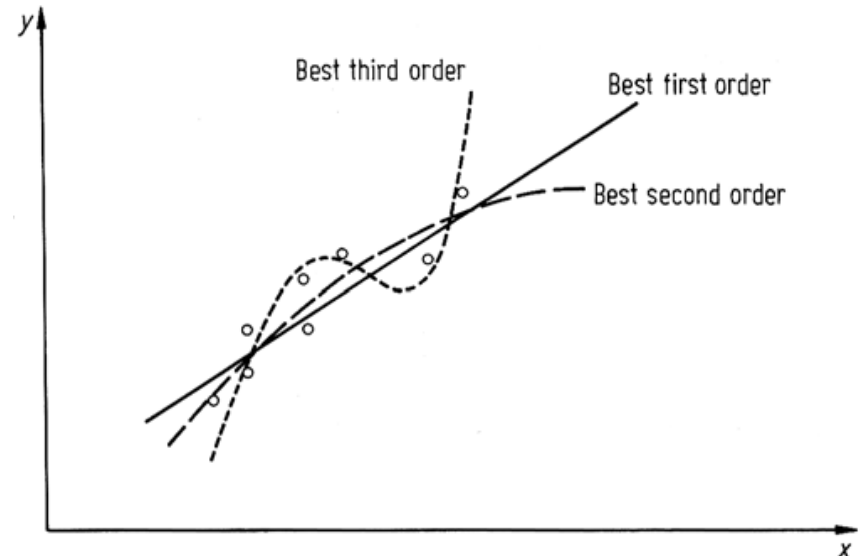
$$\phi(i + 1 + i', j + 1 + j') = i' \{ i' [\phi(i + 3, j + 1 + j') - \phi(i + 2, j + 1 + j') \\ + \phi(i + 1, j + 1 + j') - \phi(i, j + 1 + j')] \\ + [\phi(i + 2, j + 1 + j') - \phi(i + 3, j + 1 + j') \\ - 2\phi(i + 1, j + 1 + j') + 2\phi(i, j + 1 + j')] \\ + [\phi(i + 2, j + 1 + j') - \phi(i, j + 1 + j')] \} \\ + \phi(i + 1, j + 1 + j')$$

- **Cubic convolution interpolation, or resampling, yields an image product that is generally smooth in appearance and is often used if the final product is to be treated by photo-interpretation.**
- However since it gives pixels on the display grid, with brightnesses that are interpolated from the original data, it is not recommended if classification is to follow since the new brightness values may be too different from the actual radiance values detected by the satellite sensors.

Use of Mapping Polynomials for Image Correction

Choice of Control Points

- Enough well defined control point pairs must be chosen in rectifying an image to ensure that accurate mapping polynomials are generated.
- However care must also be given to the locations of the points.
 - A general rule is that there should be a distribution of control points around the edges of the image to be corrected with a scattering of points over the body of the image.
 - This is necessary to ensure that the mapping polynomials are well-behaved over the image.
- This concept can be illustrated by considering an example from curve fitting.
 - While the nature of the problem is different the undesirable effects that can be generated are similar. In Figure is illustrated a set of data points in a graph through which first order (linear), second order and third order curves are depicted.
 - Note that as the order is higher the curves pass closer to the points.
 - In contrast the cubic curve can deviate markedly from the trend when used as an extrapolator, and the linear fit seem to be the most acceptable one in this case.



Mathematical Modelling

- If a particular distortion in image geometry can be represented mathematically, then the mapping functions $u = f(x, y)$ and $v = g(x, y)$ can be specified explicitly.
- This avoids the need to choose arbitrary polynomials and to use control points to determine the polynomial coefficients
- In the following some of the more common distortions are treated from this point of view.
- However, rather than commence with expressions that relate image coordinates (u, v) to map coordinates (x, y) it is probably simpler conceptually to start the otherway around, i.e. to model what the true (map) positions of pixels should be, given their positions in an image.
- This expression can then be inverted if required to allow the image to be resampled on to the map grid.

Mathematical Modelling

Aspect Ratio Correction

- The easiest source of distortion to model is that caused by the 56 m equivalent ground spacing of the 79 m \times 79 m equivalent pixels in the Landsat MS scanner.
 - As noted this leads to an image that is too wide for its height by a factor of $79/56 = 1.411$.
 - Consequently to produce a geometrically correct image either the vertical dimension has to be expanded by this amount or the horizontal dimension must be compressed.
 - We will consider the former. This requires that the pixel axis horizontally be left unchanged but that the axis vertically be scaled. This can be expressed conveniently in matrix notation as

$$\begin{bmatrix} x \\ y \end{bmatrix} = \begin{bmatrix} 1 & 0 \\ 0 & 1.411 \end{bmatrix} \begin{bmatrix} u \\ v \end{bmatrix}$$

- and this can be inverted in

$$\begin{bmatrix} u \\ v \end{bmatrix} = \begin{bmatrix} 1 & 0 \\ 0 & 0.709 \end{bmatrix} \begin{bmatrix} x \\ y \end{bmatrix}$$

- Thus, as with the techniques based on control points, a display grid is defined over the map (with coordinates (x, y)) and the above transform is used to find the corresponding location in the image (u, v) . The already seen interpolation techniques are then used to generate brightness values for the display grid pixels.

Mathematical Modelling

Earth Rotation Skew Correction

- To correct for the effect of earth rotation it is necessary to implement a shift of pixels to the left that is dependent upon the particular line of pixels, measured with respect to the top of the image.
 - Their line addresses as such (v) are not affected.
 - From what we have already seen, these corrections are implemented by

$$\begin{bmatrix} x \\ y \end{bmatrix} = \begin{bmatrix} 1 & \alpha \\ 0 & 1 \end{bmatrix} \begin{bmatrix} u \\ v \end{bmatrix}$$

with $\alpha = -0.056$ for Sydney, Australia.

- This can be implemented in an approximate sense by making one-pixel shift to the left every 17 lines of image data measured down from the top, or alternatively, and more precisely, the expression can be inverted to give

$$\begin{bmatrix} u \\ v \end{bmatrix} = \begin{bmatrix} 1 & -\alpha \\ 0 & 1 \end{bmatrix} \begin{bmatrix} x \\ y \end{bmatrix} = \begin{bmatrix} 1 & 0.056 \\ 0 & 1 \end{bmatrix} \begin{bmatrix} x \\ y \end{bmatrix}$$

which again is used with an interpolation procedures to generate display grid pixels.

Mathematical Modelling

Image Orientation to North-South

- Although ~~not~~ strictly a geometric distortion it is an inconvenience to have an image that is ~~corrected~~ for most major effects but is not oriented vertically in a north-south direction.
 - It will be recalled for example that the Landsat orbits in particular are inclined to the north-south line by about 9° . (This of course is different with different latitudes).
- To rotate an image by an angle ζ in the counter -or anticlockwise direction (as required in the case of Landsat) it is easily shown that

$$\begin{bmatrix} x \\ y \end{bmatrix} = \begin{bmatrix} \cos \zeta & \sin \zeta \\ -\sin \zeta & \cos \zeta \end{bmatrix} \begin{bmatrix} u \\ v \end{bmatrix}$$


so that

$$\begin{bmatrix} u \\ v \end{bmatrix} = \begin{bmatrix} \cos \zeta & -\sin \zeta \\ \sin \zeta & \cos \zeta \end{bmatrix} \begin{bmatrix} x \\ y \end{bmatrix}$$


Mathematical Modelling

Correction of Panoramic Effects

- The discussion about panoramic distortion makes note of the pixel positional error that results from scanning with a fixed IFOV at a constant angular rate. In terms of map and image coordinates, the distortion can be described by

$$\begin{bmatrix} x \\ y \end{bmatrix} = \begin{bmatrix} \tan \theta / \theta & 0 \\ 0 & 1 \end{bmatrix} \begin{bmatrix} u \\ v \end{bmatrix}$$

- where ϑ is the instantaneous scan angle, which in turn can be related to x or u , namely $x = h \tan \vartheta$, $u = h\vartheta$, where h is altitude (in this case u means undistorted, i.e. proportional to ϑ).
- Consequently, resampling can be carried out according to

$$\begin{bmatrix} u \\ v \end{bmatrix} = \begin{bmatrix} \theta \cot \theta & 0 \\ 0 & 1 \end{bmatrix} \begin{bmatrix} x \\ y \end{bmatrix} = \begin{bmatrix} h/x \tan^{-1}(x/h) & 0 \\ 0 & 1 \end{bmatrix} \begin{bmatrix} x \\ y \end{bmatrix}$$

Mathematical Modelling

Combining the Corrections

- Clearly any exercise in image correction usually requires several distortions to be rectified.
 - Using the mapping polynomials techniques for image correction it is assumed that all sources are rectified simultaneously.
 - When employing mathematical modeling, a correction matrix has to be devised for each source considered important, as in the preceding slides, and the set of matrices combined.
 - For example, if the aspect ratio of a Landsat TM image is corrected first, followed by correction of the effect of earth rotation, then the following single linear transformation can be established for resampling

$$\begin{bmatrix} x \\ y \end{bmatrix} = \begin{bmatrix} 1 & \alpha \\ 0 & 1 \end{bmatrix} \begin{bmatrix} 1 & 0 \\ 0 & 1.411 \end{bmatrix} \begin{bmatrix} u \\ v \end{bmatrix}$$
$$= \begin{bmatrix} 1 & 1.411\alpha \\ 0 & 1.411 \end{bmatrix} \begin{bmatrix} u \\ v \end{bmatrix}$$

which for $\alpha = -0.056$ (at Sydney) gives

$$\begin{bmatrix} u \\ v \end{bmatrix} = \begin{bmatrix} 1 & 0.056 \\ 0 & 0.709 \end{bmatrix} \begin{bmatrix} x \\ y \end{bmatrix}$$

Georeferencing and Geocoding

- Using the correction techniques of the preceding sections an ~~image~~ can be registered to a map coordinate system and therefore have its pixels addressable in terms of **map coordinates** (eastings and northings, or latitudes and longitudes) rather than pixel and line numbers.
- **Other spatial data types**, such as geophysical measurements, image data from other sensors and the like, can be registered similarly to the map thus creating a **georeferenced integrated spatial data base** of the type used in a **geographic information system (GIS)**.

any image can be
registered to map data

□ **Nomenclature**

- **Image to image registration:** the alignment of an image (slave) to another image (master) of the same area (e.g. taken at different dates and/or with different techniques)
- **Rectification or georeferencing:** the alignment of an image to a map (also by geometric distortion correction, in this case we refer to an *orthorectification*) so that the image is *planimetric*, just like the map.
- A particular rectification which allow to directly express image pixel addresses in terms of a map coordinate base is often referred to as *geocoding*.

Image to Image Registration

- Many applications of remote sensing image data require *two or more scenes of the same geographical region, acquired at different dates, to be processed together.*
 - Such a situation arises for example when **changes** are of interest, in which case registered images allow a *pixel-by-pixel comparison* to be made. [i.e. when the ground changes somehow]
- Two images can be registered to each other by registering each to a map coordinate base separately, in the manner demonstrated previously.
- Alternatively, and particularly if georeferencing is not a priority, one image can be chosen as a **master** to which the other, known as the **slave**, is to be registered.
 - Again the already seen techniques are used, however
 - the coordinates (x, y) are now the pixel coordinates in the master image rather than the map coordinates;
 - while, as before, (u, v) are the coordinates of the image to be registered (i.e. the slave).
- An advantage in *image-to-image* registration is that *only one registration step is required* in comparison to *two* if both are taken back to a map base.

Image to Image Registration

- Manual **GCP selection** and **correspondence search** between two images (or between one image and a map) can be a tedious and time-consuming task
- Today there are several solutions (**feature-point extraction and description techniques**) that allow the latter task or even both to be automatic or semiautomatic (~~with reasonable reliability and robustness~~)

GCP Selection.

- Following, a possible *classification* of automatic or semiautomatic image-to-image registration or GCP localization and correspondence search techniques:
 - Algorithms that uses pixel intensity values directly (rigid or affine registration)
 - Correlation methods
 - Mutual information maximization methods
 - Frequency- or wavelet-domain techniques (rigid or affine registration)
 - **Feature-based methods** that uses *low-level features* such as shapes, edges and corners (both rigid and deformable registration)
 - comprising both manually or semi-automatically selected feature points, like GCPs
 - or automated ones, like SIFT
 - Object-based (*high-level features*) techniques (less used for registration)

Control Point Localisation by Windowed Image Correlation

- To locate the position of a control point in the master image, having identified it in the slave, **(localized) correlation techniques** can be used.
 - The *correlation measure used need not be sophisticated*: a simple similarity check that can be used is to compute the sum of the absolute differences of the slave and master image pixel brightnesses over a local window (around the control point), for each possible location of the window in the search region.
 - In principle a rectangular sample of pixels surrounding the control point in the slave image can be extracted as a window to be correlated with the master image.
 - Because of the spatial properties of the pair of images near the control points a high correlation should occur when the slave window is located over its exact counterpart region in the master, and thus the master location of the control point is identified.
 - Obviously, it is not necessary to move the slave window over the complete master image since the user knows approximately where the control point should occur in the master.
 - Consequently, it is only necessary to specify a search region in the neighborhood of the approximate location.
 - In remote sensing this is also called **sequential similarity detection algorithm (SSDA)** ~~[Bernstein (1983)]~~
 - Clearly the use of techniques such as these to locate control points depends upon there not being major changes of an uncorrelated nature between the scenes in the vicinity of a control point being tested.

Example of Image to Image Registration (manual GCP selection - SSDA)

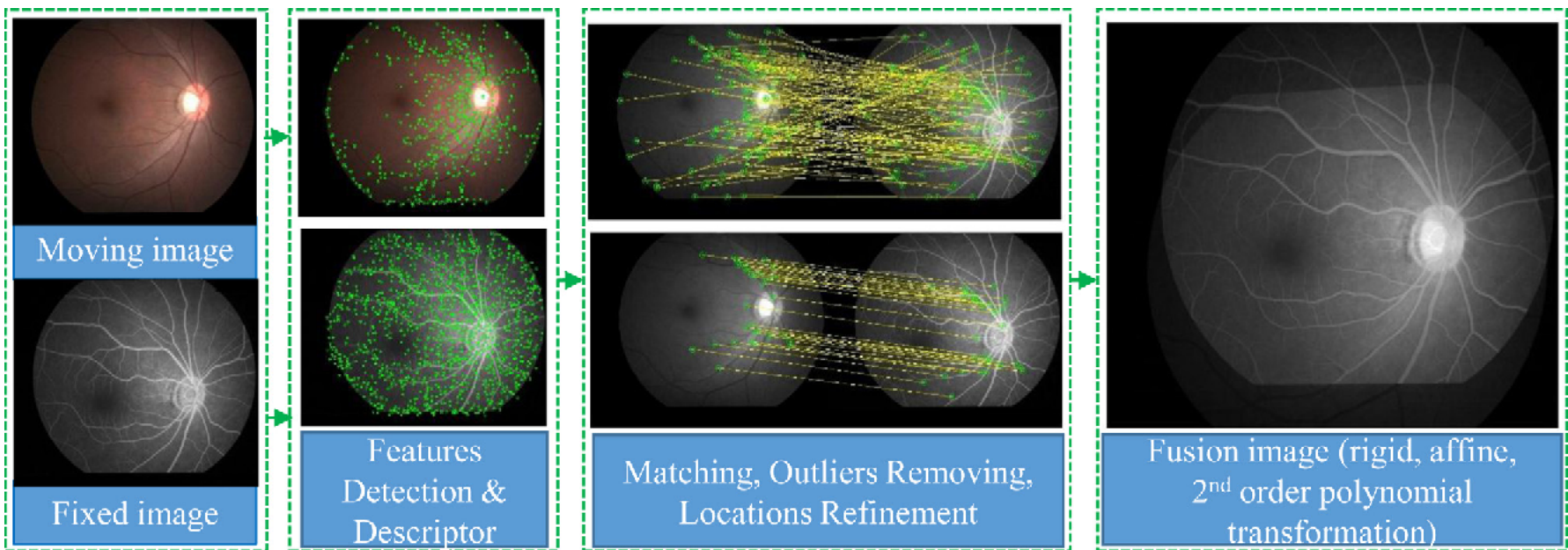
- We exemplify **image to image registration**, and more particularly
 - we see clearly the effect of control point distribution and
 - the significance of the order of the mapping polynomials to be used for registration
- Two segments of *Landsat MSS infrared image data* in the northern suburbs of Sydney were chosen:
 - one was acquired on December 29, 1979 and was used as the master;
 - the other was acquired on December 14, 1980 and was used as the slave image.
- ***Two sets of control points*** were chosen.
 1. In one the points were distributed as nearly as possible in a uniform manner around the edge of the image segment as shown in the following Figure (a), with some points located across the centre of the image.
 2. The second set of control points was chosen injudiciously, closely grouped around one particular region, to illustrate the resampling errors that can occur (see Figure (b)).
 - In both cases the control point pairs were co-located with the assistance of a sequential similarity detection algorithm (**correlation based**).
 - This worked well particularly for those control points around the coastal and river regions where the similarity between the images is unmistakable.
 - *Data curation hint!* To minimize tidal influences on the location of control points, those on water boundaries were chosen as near as possible to be on headlands, and certainly were never chosen at the ends of inlets.

Examples of Image to Image Registration (manual GCP selection - SSDA)

- The adequacy of the **registration process** can be assessed visually if the master and resampled slave images can be **superimposed in different colors**.
 - The following figures show the master image in *red* with the resampled slave image superimposed in *green*.
 - Where **good registration** has been achieved the resultant is **yellow** (with the *exception* of regions of gross dissimilarity in pixel brightness – in this case associated with *fire burns*).
 - Misregistration shows quite graphically by a red-green separation.
- For both sets of control points ***third degree mapping polynomials*** were used along with ***cubic convolution resampling***.
 - As expected the first set of points led to an acceptable registration of the images (Figure a) whereas the second set gave a good registration in the immediate neighborhood of the points but beyond them produced gross distortion (Figure b), which is particularly noticeable (red-green separation) when the poor extrapolation obtained with third order mapping is demonstrated.
- The registration using the poor set of control points was repeated, this time only ***first order mapping polynomials*** were used.
 - While these obviously *will not remove non-linear differences between the images* and will give poorer matches at the control points themselves, they are well behaved in extrapolation beyond the vicinity of the control points and lead to an *acceptable registration*, as shown in Figure c.

Control Point Localisation by automated Feature Extraction and Matching

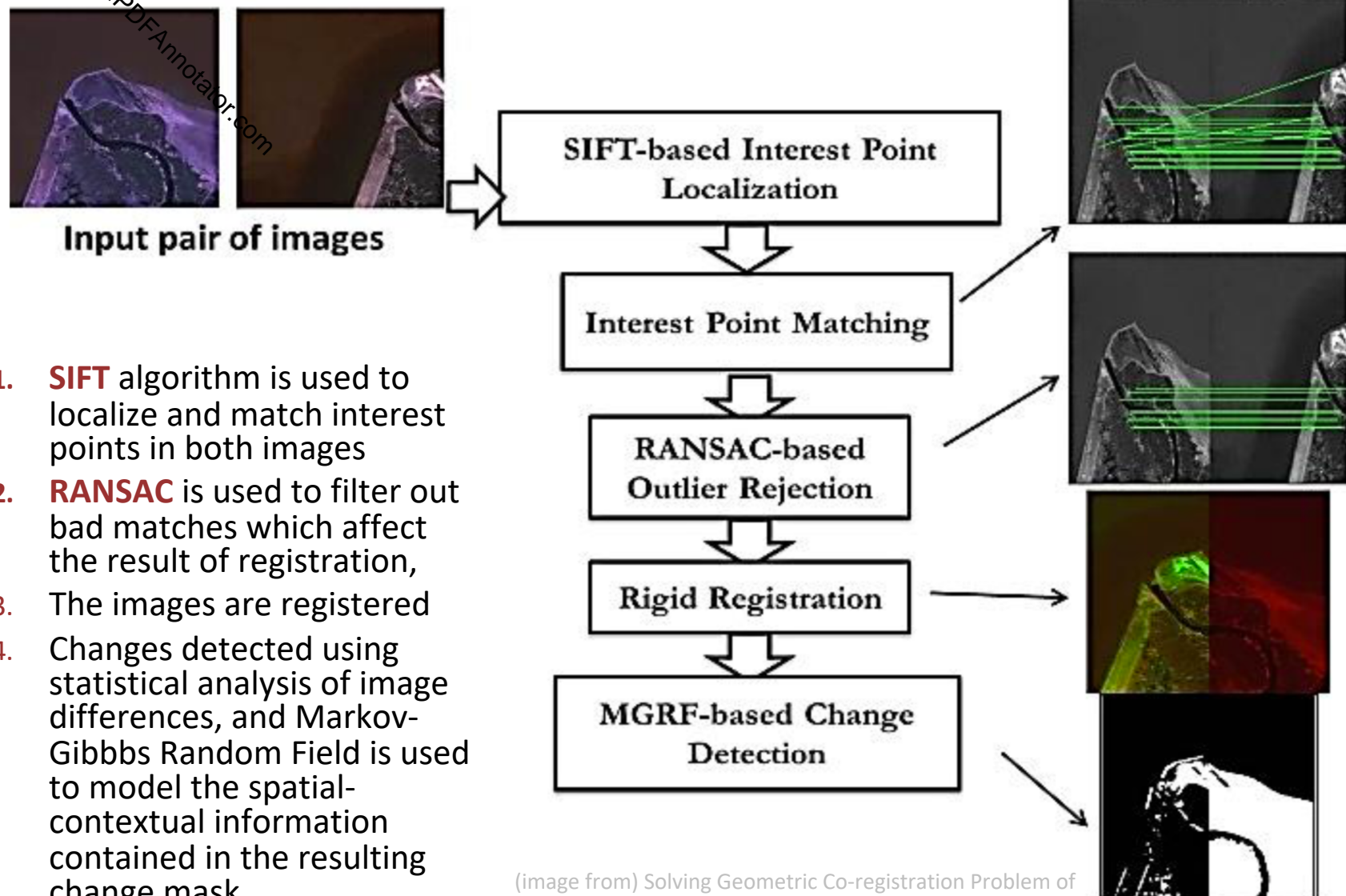
- Modern **feature based methods** can lead to more automated GCP localization both in the slave and master images, to produce more effective image to image registrations.
 - Rotation, translation (and possibly scale) *invariant feature* search must be considered to be robust to geometric distortions
 - Feature sets are extracted from both the master and the slave images (or map and image)
 - Each feature is described by its geometric (geographic in the case of a map) position and an associated *signature*, i.e. a discriminative vector computed on the feature neighborhood.
 - **Correspondences** (matching) between couples of features in the master and slave images can be defined. Their potential number (combination) is very high but only a few are correct.
 - Registration transform is defined upon reliable feature correspondences.



Control Point Localisation by automated Feature Extraction and Matching

- Modern **feature based methods** can lead to more automated GCP localization both in the slave and master images, to produce more effective image to image registrations
 - Rotation, translation (and possibly scale) *invariant feature* search must be considered to be robust to geometric distortions
 - Feature sets are extracted from both the master and the slave images (or map and image)
 - Each feature is described by its geometric (geographic in the case of a map) position and an associated **signature**, i.e. a discriminative vector computed on the feature neighborhood.
 - **Correspondences** (matching) between couples of features in the master and slave images can be defined. Their potential number (combination) is very high but only a few are correct.
 - Registration transform is defined upon reliable feature correspondences (after outlier removal).
- Correspondence test procedures (feature matching + outlier removal) are of critical importance in order to determine, in a reliable and robust way, a set of correct correspondences which in turn define the associated set of ground control points.
- Various correspondence test approaches can be envisaged
 - Brute force methods (e.g. **RANSAC** technique, Fisher&Bolles 1981), based on feature point positions
 - **Feature description** methods (e.g. based on SIFT), based on signature similarity measures
 - *Mixed approaches*: for example, correspondences are first ranked and then skimmed based on signature similarity and then validated through tests based on geometric constraints (or viceversa) – or **correspondences are initially estimated by feature similarity measures and then consensus based statistical analysis (RANSAC) is used to reject outliers and estimate registration transform** (see example below).

Example of Image to Image Registration (automated feature based)



1. **SIFT** algorithm is used to localize and match interest points in both images
2. **RANSAC** is used to filter out bad matches which affect the result of registration,
3. The images are registered
4. Changes detected using statistical analysis of image differences, and Markov-Gibbs Random Field is used to model the spatial-contextual information contained in the resulting change mask

(image from) Solving Geometric Co-registration Problem of Multi-spectral Remote Sensing Imagery Using SIFT-Based Features toward Precise Change Detection – ISVC 2011